Atmospheric Research 181 (2016) 220–235

Contents lists available at ScienceDirect

Atmospheric Research

journal homepage: www.elsevier.com/locate/atmosres

The 20th century transitions in basic and extreme monsoon rainfall indices in India: Comparison of the ETCCDI indices

Dileep K. Panda *, P. Panigrahi, S. Mohanty, R.K. Mohanty, R.R. Sethi

Indian Institute of Water Management (ICAR-IIWM), Chandrasekharpur, Bhubaneswar 751023, Odisha, India

ARTICLE INFO

Article history:
Received 10 March 2016
Received in revised form 1 July 2016
Accepted 5 July 2016
Available online 06 July 2016

Keywords:
Extreme rainfall indices
Spatiotemporal pattern
Indian monsoon season
PDSI
TIO SST

ABSTRACT

The mean and extreme matrices of the monsoon rainfall in India not only play an important role in depicting the global monsoon climate, but also their spatiotemporal patterns influence the socio-economic profile of a major proportion of the country's huge population. Given the reported conflicting trends at the global and national scales, the present study investigates the 20th century (1901–2004) changes in monsoon rainfall of India, particularly focusing the indices developed by the Expert Team on Climate Change Detection and Indices (ETCCDI) to facilitate a global comparison. Result of this comprehensive analysis, which includes the response of fifteen indices over two study periods (i.e., 1901–1940 and 1961–2004), indicates clear signals of change with respect to the period and region of study and the choice of the ETCCDI indices. While wet day frequency, low-to-moderate events and consecutive wet days (CWD) exhibit a prominent transition from a pre-1940 wetting to a post-1960 drying tendency over a large part of the central-north India (CNI), both the wet and dry extremes have occurred in a spatially less consistent manner during the recent decades. For consecutive dry days (CDD), the reported less clear global signals could be related to the timescale of analysis, as our sub-seasonal scale results display consistent changes compared to that of the seasonal and annual scales. The Palmer Drought Severity Index (PDSI) provides clear indications of a post-1960 non-stationarity, showing changes in the mean as well as variance. Based on the partial Mann–Kendall test (PMK), some of the identified rainfall trends during 1961–2004 are found to be influenced more by the tropical Indian Ocean sea surface temperatures than the El Niño–Southern Oscillation index. These results have important implications for formulating the water resource management strategy, particularly over the drying central and northern parts of the country.

1. Introduction

The south Asian countries, home to about one-fifth of the world's population, rely heavily upon the summer monsoon rainfall during June to September for their socio-economic welfare and environmental sustenance. However, erratic spatiotemporal distributions in the form of extreme rainfall events, as illustrated in the recent Intergovernmental Panel on Climate Change (IPCC) Fifth Assessment Report (Stocker et al., 2013), have been causing immense economic losses, including the loss of human beings. Given the profound implications of the summer monsoon rainfall, several research efforts have been undertaken in the recent past, reflecting substantial spatial variations of the statistically significant rainfall trends (Turner and Annamalai, 2012). The 21st century projected increases in both wet and dry extremes, particularly at a higher rate over the Asian monsoon region due to anthropogenic warming induced intensification of the monsoon rainfall (Kitoh et al., 2013; Krishnan et al., 2013). The potential response of the Indian monsoon circulation, identified as a complex feature of the global climate system, poses challenges of both scientific and societal interest because of its influence on the economy by providing subsistence to nearly two-third of the country's over 1.2 billion population (Revadekar and Preethi, 2012).

The global mean monsoon rainfall has experienced multidecadal variations during the 20th century (1901–2001), with an overall increasing pattern up to 1955 driven particularly by the increases over the North African, Indian and East Asian monsoon belt, and followed by a decreasing pattern up to 2001 (Zhang and Zhou, 2011). In general, a weakening of the monsoon during the second half of the 20th century has been reported by several other studies (Zhou et al., 2008; De Luis et al., 2009; Wang et al., 2012). Consistently, the Indian monsoon rainfall has increased (decreased) during the first (second) half, resulting in no apparent trend in the century-scale analysis (Joshi and Pandey, 2011; Turner and Annamalai, 2012). Several global studies provide clear indications of warming induced increases in frequency and intensity of extreme rainfall since the 1950s (Stocker et al., 2013; Westra et al., 2013; Zhang et al., 2013).

* Corresponding author.
E-mail address: dileeppanda@rediffmail.com (D.K. Panda).

http://dx.doi.org/10.1016/j.atmosres.2016.07.002
0169-8095/

During the post-1950 period, the Indian summer monsoon rainfall shows a complex spatiotemporal and intra-seasonal pattern in its mean and extreme measures. While the aggregated daily rainfall (R) over central India has displayed a rise in the frequency and intensity of heavy (R70/R100, $R > 70/100$ mm) and very heavy rain events (R150, $R > 150$ mm), along with decreases in the low-to-moderate rainfall events (LMR, 5 mm $< R \leq 100$ mm) in the background of an warming environment (Goswami et al., 2006; Rajeevan et al., 2008; Dash et al., 2009), a robust drying signal from the weakened monsoon circulation is also reported for the same region due to the likely influence of the south Asian aerosol emissions (Bollasina et al., 2011).

Preceding the 1950s, assessment of changes in rainfall extremes has not been possible in many parts of the world because of scarcity in high resolution daily records (Alexander et al., 2006), for which understanding on multidecadal changes in extreme climate over the entire past century remains less explained (Moberg et al., 2006; Griffiths and Bradley, 2007). Using a newly updated observational dataset with improved spatial and temporal coverage since the beginning of the 20th century, Donat et al. (2013) assessed the global patterns of climatic indices developed by the Expert Team on Climate Change Detection and Indices (ETCCDI). Although they observed more areas with significant increasing trends in extreme rainfall, a less clear signal has emerged for some of the indices, such as the heavy rainfall intensity (i.e., maximum 5-day rainfall total, Rx5day) and also in dry spell lengths (i.e., maximum number of consecutive dry days, CDD). It can also be noticed that R10 ($R > 10$ mm), defined by the ETCCDI as a heavy rainfall event, has decreased uniformly over central-north India (CNI), which appears to be the reflection of the LMR (low-to-moderate rainfall events) tendency, based on the LMR definition of the Indian monsoon climate. Some continental and country-specific assessments of the twentieth century changes in extreme rainfall include the following: Moberg et al. (2006) for Europe, Kunkel et al. (2003) and Griffths and Bradley (2007) for the USA, Gallego et al. (2011) for the Iberian Peninsula, Brunetti et al. (2004) for Italy, Gallant and Karoly (2010) for Australia, and Villafuerte et al. (2015) for the Philippines. Results of these studies suggest that the whole 20th century contains some important information, which has not been reflected in the post-1950 changes.

For the Indian subcontinent, however, the existing studies focusing on extreme indices for the whole 20th century are very few, particularly in the context of a large spatial and temporal variability of the monsoon rainfall. But, valuable contributions have been made with respect to the analysis of mean rainfall on seasonal or annual scales for different states (e.g., Subash et al., 2011; Patra et al., 2012; Duhan and Pandey, 2013; Panda et al., 2013; Goyal, 2014; Pingale et al., 2014). For the whole country, Sen Roy and Balling (2004) assessed the linear regression trends for six extreme rainfall (Rx1day, Rx5day, Rx30day, 90th, 95th, and 97.5th percentiles) frequencies using daily rainfall over 129 stations for the period 1910–2000, revealing decreases in the eastern part of the Gangetic Plain and increases in the southern peninsular region of India. In homogeneous regions of India, Guhathakurta et al. (2015) reported a multidecadal variability of different phases in the monthly rainfall datasets during 1901–2011, while the core monsoon region experienced significant decreases in the moderate rainfall events (i.e., LMR) but no change in R100 and R150 during 1951–2010. In central India, however, Rajeevan et al. (2008) observed increases in R150 during 2001–2004. Comparing the pre- and post-1950 extreme rainfall events, Vittal et al. (2013) attributed the changes in the post-1950 period to the impacts of rapid urbanization. In contrast, Ali et al. (2014) noted no such trends during 1901–2010, considering four different measures extreme rainfall. In the Himalayan domain of the northeast India, Singh and Goyal (2016) highlighted the influence of elevation on the mean and extreme measures of rainfall. Spatially and sub-seasonally less consistent patterns reported in the literature particularly due to use of different study period, datasets, spatial domains and varying definitions of extreme rainfall (Ghosh et al., 2012; Panda and Kumar, 2014) underscore the importance of our current effort to undertake a comprehensive assessment.

Therefore, the purpose of this study is to examine the spatiotemporal and regional transitions of the 20th century monsoon rainfall in India using a multitude of statistical measures that encompass the basic rainfall characteristics, threshold- and percentile-based extreme measures, and duration-based dry and wet spells, mostly defined by the ETCCDI. Since statistical detection of extreme rainfall events is more challenging because of its inherent quality of local occurrences, non-Gaussianity and large interannual variability, it is advisable, in general, to investigate a wide range of rainfall diagnostics from a dense observational network (Groisman et al., 2005; Schmidli and Frei, 2005). Therefore, a suit of indices are examined in this study using a high-resolution uniformly gridded daily rainfall dataset during 1901–2004, thus avoiding the pre-1950 period influence of the irregular station density as highlighted by Sen Roy and Balling (2004) and Klein Tank et al. (2006).

Several previous studies have clearly indicated the varied response of the extreme rainfall indices, particularly defined by the ETCCDI, to natural modes of climate variability in different parts of the world (Kenyon and Hegerl, 2010). For India, however, response of the mean monsoon rainfall is studied extensively (e.g., Joshi and Pandey, 2011), although more understanding is required on how the ocean forcing mechanisms influence their extreme states. During 1901–2004, Rajeevan et al. (2008) observed that the interdecadal variability and trend of the central India R150 is modulated by the tropical Indian Ocean sea surface temperature (TIO SST). Extending to other ETCCDI indices, the current study investigates the potential influence of local as well as remote SST forcing on trends of the 20th century monsoon extremes. We examine the trend and variability for the sub-periods 1901–1940 and 1961–2004, which coincides with the two major warming phases of the 20th century, separated by a cooling period (i.e., 1941–1960). This will provide important insights about the transition in monsoon rainfall characteristics under two contrasting background, as far as anthropogenic warming is concerned. Given the 21st century uncertainty in the model projections of the mean monsoon rainfall and the ETCCDI indices (Kitoh et al., 2013; Saha et al., 2014; Hasson et al., 2016), this paper presents for the first time a full picture of the century scale (i.e., 1901–2004) changes in the ETCCDI indices in India, which should serve as an useful observational baseline for the future model projection and validation.

In the following section, the datasets and indices are described. Section 3 presents the methodology. The results are discussed in Section 4, and concluding remarks are made in Section 5.

2. Dataset and extreme indices

The daily gridded rainfall dataset employed in this study for the period 1901–2004 at a spatial resolution of 1° latitude × 1° longitude has been developed by the India Meteorological Department (IMD) employing the Shepard's interpolation method. The observed rainfall data from >1800 gauges was used to develop this gridded dataset, and multi-stage quality control steps were followed to minimize temporal inhomogeneity due to varying station densities, which is detailed in Rajeevan et al. (2008). We opt this dataset over that of the recently updated rainfall dataset at a spatial resolution of 0.25° latitude × 0.25° longitude, because the employed dataset is validated with a range of applications in climate assessment studies until now (e.g., Rajeevan et al., 2008; Joshi and Pandey, 2011; Krishnamurthy and Krishnamurthy, 2013; Vittal et al., 2013). Moreover, our results can be compared with the previous ones without anticipated bias from different datasets. For a more recent qualitative comparison of IMD rainfall datasets at different spatial resolutions, Guhathakurta et al. (2015) may be referred. To calculate the monsoon rainfall indices defined in Table 1, the time series from 306 evenly distributed grids over the Indian subcontinent are used.

Table 1
List of rainfall indices used in this study for the monsoon season (June to September).

Category	Index	Definition	Unit
Absolute indices	Rx1day	Maximum 1-day rainfall total	mm
	Rx5day	Maximum 5-day rainfall total	mm
Threshold indices	R70/100/150 (nn)	Number of days with rainfall 70/100/150 mm or more	Days
Duration indices	CWD	Consecutive wet days. Maximum number of consecutive wet days (i.e. when $R \geq 1$ mm)	Days
	CDD	Consecutive dry days. Maximum number of consecutive dry days (i.e. when $R < 1$ mm)	Days
Percentile-based indices	R95p	Very wet days. Total rainfall due to events exceeding the 95th percentile of the 1961–1990 base period	mm
	R99p	Extremely wet days. Total rainfall due to events exceeding the 99th percentile of the 1961–1990 base period	mm
	R95pTOT	Contribution from very wet days. Fraction of total rainfall due to events exceeding the 95th percentile of the 1961–1990 base period	%
	R99pTOT	Contribution from extremely wet days. Fraction of total rainfall due to events exceeding the 99th percentile of the 1961–1990 base period	%
Basic indices	WD	Wet days. Number of days with rainfall (R) of ≥1 mm	Days
	PRCPTOT	Total rainfall (precipitation) on days with ≥1 mm rain	mm
	LMR	Low-to-moderate rainfall events. Number of days with rainfall between 5 mm and 100 mm (i.e. 5 mm $< R \leq$ 100 mm)	Days
	SDII	Simple daily intensity index. Total rainfall divided by the number of wet days (i.e. average rainfall of the on days with rainfall ≥1 mm)	mm day^{-1}

Full definitions are available from the ETCCDI website http://cccma.seos.uvic.ca/ETCCDI/.

The SST-based indices are derived from the National Oceanic and Atmospheric Administration National Climate Data Center (NOAA NCDC) monthly Extended Reconstructed Sea Surface Temperature version 3 dataset (ERSST.v3b) (Smith et al., 2008). Specifically, we construct TIO SST index by averaging the SST anomalies over the tropical Indian Ocean (20° S–30° N, 50–120° E), and the El Niño–Southern Oscillation (ENSO) index by averaging the monsoon season SST anomalies over the NINO3.4 region (5° S–5° N, 170°–120° W). These two indices are widely used in the literature to link variations of the monsoon rainfall.

Consistent with the ETCCDI definitions of extreme indices in Table 1 (Zhang et al., 2011; Donat et al., 2013), daily rainfall (R) ≥ 1 mm in the monsoon season (June to September) is considered as a wet day and below this value is a dry day, while comparisons with the IMD defined wet day ($R \geq 2.5$ mm) yield no apparent difference. The extreme wet and dry rainfall indices investigated in this study (Table 1) fall roughly into five different categories as presented in Alexander et al. (2006). Nevertheless, the threshold-based frequency of heavy (R10) and very heavy rainfall events (R20) are replaced by the corresponding appropriate definition of R70, R100 and R150 for India (i.e., Rnn, monsoon count of rainfall above a user-defined threshold). In order to spatially compare the extreme rainfall within the diverse climatology of India (Fig. 1) and also for the international comparisons, the percentile-based rainfall intensity, such as the total rainfall from very and extreme wet days (R95p and R99p) (i.e., above the 95th and 99th percentile of the base period 1961–1990), have relative advantage over the fixed thresholds

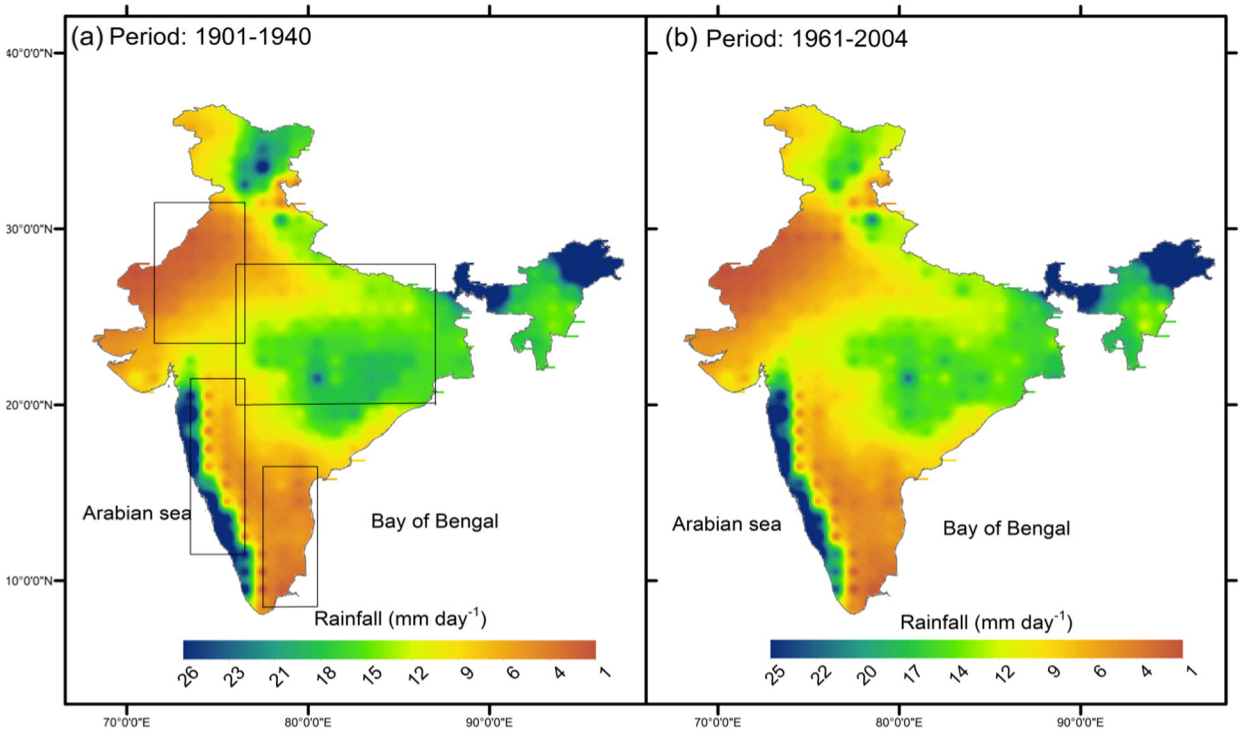

Fig. 1. Spatial pattern of the mean monsoon (June–September) rainfall rates (mm day^{-1}) during the (a) 1901–1940 and (b) 1961–2004 periods in India. The central-northern India (CNI), indicated by the box (20°–28° N, 76°–87° E), encompassing parts of the core monsoon belt and the Ganga River basin, shows a noticeable rainfall decline during the recent period. Other regions indicated by boxes are the northwest India (NWI), southwest India (SWI) and southeast India (SEI).

indices (Klein Tank and Können, 2003). Even if the indices R95pTOT and R99pTOT, representing the fraction of monsoon rainfall due to very and extreme wet days are not included in the ETCCDI definitions, they are identified to have significant social impacts by the Hadley Center Global Climate Extremes Index 2 (HadEX2) (Donat et al., 2013). Furthermore, the magnitude of intense rainfall events are assessed through the indices Rx1day, Rx5day and the average amount of rainfall received on wet days (i.e., SDII).

The basic rainfall characteristics, such as total monsoon rainfall from wet days (PRCPTOT), wet days frequency (WD) and low-to-moderate rainfall events (LMR), are important, since they are closely tied with the upper and lower tails (extremes) of the distribution; for example, under global warming increases in rainfall intensity concurs with increases in dry spells through decreases in WD and LMR, leading to a little or no change in the mean rainfall (PRCPTOT) (Goswami et al., 2006; Giorgi et al., 2011). Although decreases in consecutive wet days (CWD) and/or increases in consecutive dry days (CDD) reflect the length of the driest part of the monsoon season from climate change prospective, but the agricultural and hydrological droughts are directly linked to LMR. Since droughts have posed serious challenges to water resources and ecosystems of India, to supplement the above indices, we use the monthly self-calibrated Palmer Drought Severity Index (PDSI) with a spatial resolution 2.5° latitude × 2.5° longitude spanning over January 1961 to December 2010, which is a prominent index for characterization of a meteorological drought taking into account the cumulative effect of rainfall and temperature changes (Dai et al., 2004). In order to understand the contrasting regional diversity of the monsoon climatology, spatially aggregated dry and wet extremes are compared for four regions of India (Fig. 1): the central-northern India (CNI; 20°–28° N, 76°–87° E), northwest India (NWI; 23.5°–31.5° N, 71.5°–76.5° E), southwest India (SWI; 11.5°–21.5° N, 73.5°–76.5° E) and southeast India (SEI; 8.5°–16.5° N, 77.5°–80.5° E). The grid scale standardized anomalies, based on the 1961–1990 climatology, are filtered through a 10-year running mean to remove the sub-decadal variability (Joshi and Pandey, 2011), and the regionally averaged anomalies are plotted to facilitate a visual comparison of the existing multidecadal variability.

3. Methodology

3.1. Trend detection

Presence of monotonic trends in rainfall indices have been evaluated using the Mann-Kendall (MK) nonparametric test (Sneyers, 1999; Zhang et al., 2001), which does not make assumptions about the underlying distribution, and also is insensitive to effects of outliers in the extreme indices. Since world-wide analysis suggests that several extreme indices do not necessarily follow a Gaussian distribution (Alexander et al., 2006), this test is one of the most widely used statistical tests to detect the hydro-climatological signals of climate change and variability given its advantages over the standard regression trend test (e.g., Westra et al., 2013). However, the null hypothesis of the MK test requires that data (X_1, X_2, …, X_n) are a sample of n independent and identically distributed random variables.

The MK test statistics, S, is defined as

$$S = \sum_{i=1}^{n-1} \sum_{j=i+1}^{n} \mathrm{sgn}(X_j - X_i) \tag{1}$$

where X_i and X_j are the data values at times i and j of the time series of length n. The sgn is evaluated as

$$\mathrm{sgn}(\theta) = \begin{cases} +1 & \text{for} \quad \theta > 0 \\ 0 & \text{for} \quad \theta = 0 \\ -1 & \text{for} \quad \theta < 0 \end{cases} \tag{2}$$

Under the null hypothesis, for $n \geq 10$, the test statistics S is approximately normally distributed. Using a two-sided test, the trend is statistically significant at the level α if the absolute value of the standard normal variate, $|Z| > Z_{1-\alpha/2}$, where Z is given as

$$Z = \begin{cases} \dfrac{S-1}{\sqrt{\sigma_s^2}} & \text{for} \quad S > 0 \\ 0 & \text{for} \quad S = 0 \\ \dfrac{S+1}{\sqrt{\sigma_s^2}} & \text{for} \quad S < 0 \end{cases} \tag{3}$$

A positive (negative) value of Z indicates an upward (downward) trend. In this study, the significant trends are detected at the 5% and 10% significance level (i.e., p-value of ≤0.05 and 0.1) unless mentioned otherwise. Presence of serial correlation in time series has been addressed through the trend-free pre-whitening (TFPW) procedure (Yue et al., 2002). The magnitude (β) of trends is determined using the Theil–Sen approach (Zhang et al., 2001), which is also a robust non-parametric method given as

$$\beta = Median\left(\frac{X_j - X_i}{j-i}\right) \forall i < j. \tag{4}$$

We assess the common trend over the regions depicted in Fig. 1 employing the analytical method developed by Douglas et al. (2000). Using the test statistics S of individual grid points, the regional average of the MK test statistics is defined as

$$\overline{S}_m = \sum_{g=1}^{m} S_g \tag{5}$$

where S_g represents the MK test statistics for the grid g of a region with m grids. For an independent and identically distributed dataset, $\overline{S}_m$ follows a normal distribution with mean 0 and variance $\sigma_s^2 m^{-1}$, and their ratio gives the normalized test statistics Z_r. However, for a spatially correlated domain, as pointed by Kulkarni et al. (2012) for the monsoon rainfall of India, the variance of $\overline{S}_m$ becomes

$$\mathrm{Var}\left(\overline{S}_m\right) = \frac{\sigma_s^2}{m^2}\left[1 + (m-1)\overline{\rho}_{g,g+l}\right], \text{and} \tag{6}$$

$$\overline{\rho}_{g,g+l} = 2m^{-1}(m-1)^{-1} \sum_{g=1}^{m-1} \sum_{l=1}^{m-g} \rho_{g,g+l} \tag{7}$$

represents the average cross-correlation for the region (Douglas et al., 2000).

The partial Mann–Kendall test (PMK) (Libiseller and Grimvall, 2002) has been used to detect significant trends in the mean and extreme indices of monsoon rainfall after accounting the correlation with the SST-based large-scale climatic modes (i.e., TIO SST and NINO3.4 indices) as covariates. Using the conditional mean and variance of the dependent variable (rainfall indices), the PMK is computed as

$$\mathrm{PMK} = \frac{S_y - \hat{\rho} S_x}{\sqrt{\left(1-\hat{\rho}^2\right) n(n-1)(2n+5)/18}} \tag{8}$$

where S_x is the MK statistics of the covariate and S_y is the MK statistics of the dependent variable and $\hat{\rho}$ represents the correlation S_x and S_y. Under the null hypothesis, the PMK follows a normal distribution with mean 0 and standard deviation 1. A significant ($p \leq 0.1$) PMK statistics suggests that the dependent variable co-varies with the trend of the independent SST indices. Additionally, we compare with the results from the method followed by Vincent et al. (2015) that first assess the influence of the independent variables by regressing with the grid scale response

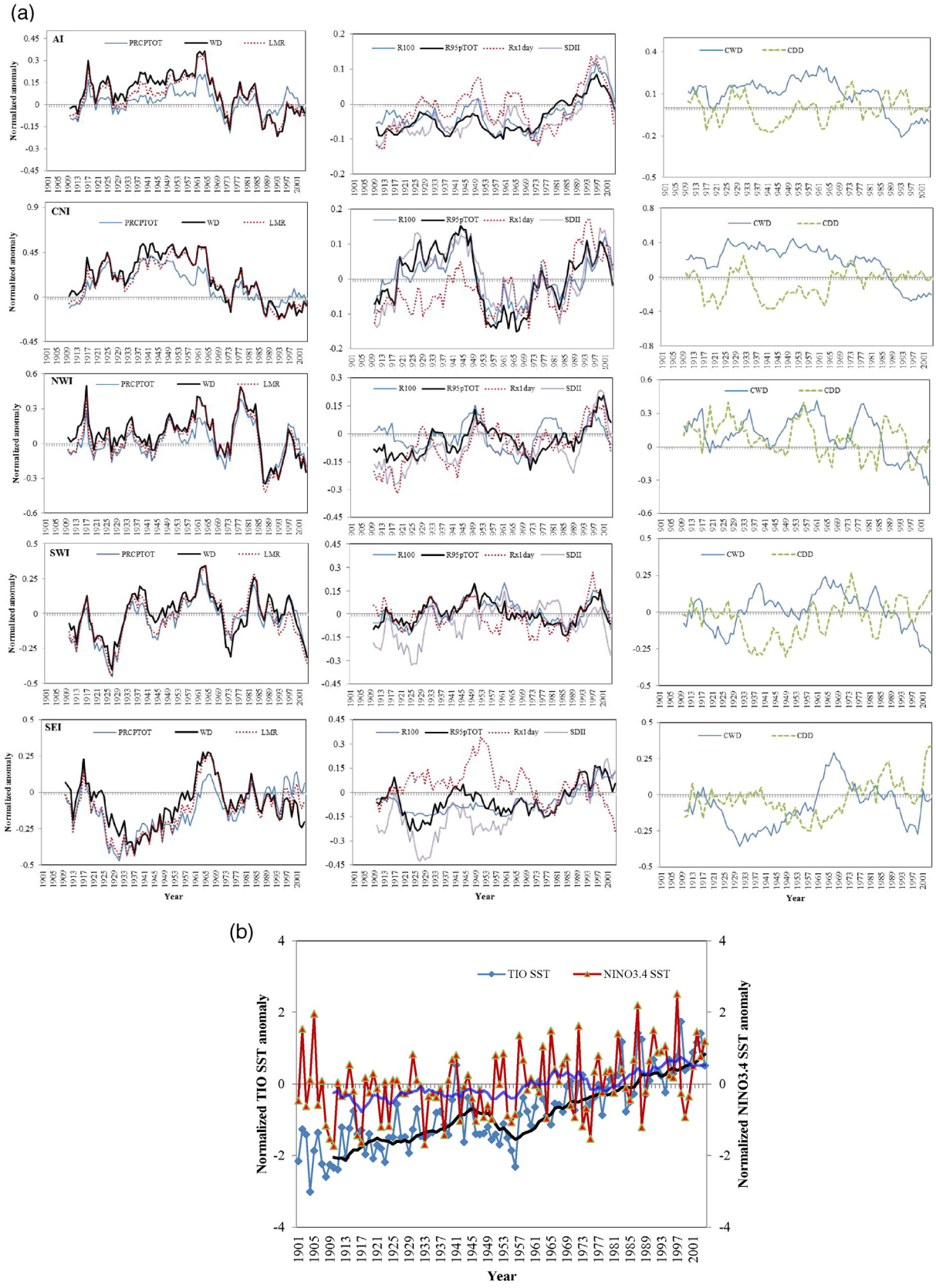

Fig. 2. (a) Time series of the 10-year running mean of normalized anomalies of the monsoon rainfall indices during 1901–2004 averaged over geographical regions: all India (AI), central-north India (CNI; 20°–28° N, 76°–87° E), northwestern India (NWI; 23.5°–31.5° N, 71.5°–76.5° E), southwest India (SWI; 11.5°–21.5° N, 73.5°–76.5° E), and southeast India (SEI; 8.5°–16.5° N, 77.5°–80.5° E), arranged in respective rows. The grid point time series are normalized by their means and standard deviations using the base period 1961–2000, and then are smoothed with a 10-year running mean to remove the subdecadal variability. (b) The monsoon season normalized SST anomalies over the tropical Indian Ocean (TIO SST; 30°N–20° S, 50° E–120° E) and over the NINO3.4 region (5° S–5° N, 170°–120° W) during 1901–2004, along with the embedded lines of the 10-year running means.

variable and then applying the MK test to the residual time series to identify trends.

Detection of trend is indicative of a non-stationary climate, which could have arisen due to a change in mean, in variability, or both. In order to better diagnose these changes, we compare the probability density function (PDF) of the pooled grid scale meteorological indices in different sub-periods of the 20th century. Furthermore, even if trends are not detected due to the high interannual and interdecadal variability of the monsoon climate, then its extreme nature can be reflected through the heavy tails in the PDFs. Significance of the difference in mean and variability has been evaluated using the Student's *t*-test and Levene's *F*-test, respectively.

4. Result and discussion

4.1. Trends in basic indices

Fig. 2a illustrates the nationally and regionally averaged normalized anomalies, with the sub-decadal variability smoothed by the 10-year moving mean, in the basic and extreme measures of the monsoon (JJAS) rainfall in India during the 20th century (1901–2004). The most interesting feature of the multidecadal oscillation is the conspicuous difference in the trend and variability between the pre-1940 (1901–1940) and the post-1960 (1961–2004) periods, which corresponds to the two observed warming phases of the TIO SST index (Fig. 2b). The basic indices (PRCPTOT, WD, LMR) appear to have two inverted-U shaped above-normal phases during the pre-1970 period, and followed by the presence of simultaneous below- and above-normal rainfall epochs (Fig. 2a), with significant ($p < 0.05$) correlation coefficients ranging from 0.70 to 0.94 for most of the regions. For the unsmoothed total monsoon rainfall (i.e., PRCPTOT), the pre-1940 (post-1960) period has experienced a significant increasing (nonsignificant decreasing) trend (Table 1), with the mean rainfall of 900 mm (896 mm) and standard deviation of 87 mm (96 mm). This nonlinear century-scale behaviour of the monsoon rainfall, with a near-neutral trend of 0.1 mm decade^{-1}, has also been earlier reported (e.g., Joshi and Pandey, 2011). The patterns observed in this study are identical to the global and Northern hemispheric land monsoon precipitation during 1901–2001 identified by Zhang and Zhou (2011) using the MK test. Therefore, this study confirms the reported major contributions of the Indian monsoon rainfall to the global monsoon trends.

Noteworthy is the substantial regional differences of the basic and extreme indices, which have not been clearly reflected in the nationally averaged time series (Fig. 2a). Whereas the northern parts of India, including central-north India (CNI) and northwest India (NWI), have experienced a nonsignificant decline in total rainfall (PRCPTOT) during 1901–2004, an opposite tendency can be noticed in southwest India (SWI) and southeast India (SEI) (Table 2). But all the four regions have a common negative trend during 1961–2004, with the largest decline of 45.98 mm decade^{-1} in the southwest region, part of the domain through which the moisture-laden monsoon wind enters the Indian subcontinent. The core monsoon region (18°–28° N, 73°–82° E), identified for having experienced a drying tendency along with high spatiotemporal variability (Singh et al., 2014), also shows a post-1960 decline of 12.81 mm decade^{-1}. In central-north India (CNI), which is a densely populated and intensely cultivated landscape encompassing of the core monsoon belt and the Ganga River basin, the monsoon rainfall has reduced from 1000 mm in the pre-1940 to 959 mm in the post-1960 period, with respective standard deviation of 104 mm and 129 mm.

Results of the grid scale trend analysis reveal no clear change in PRCPTOT during the pre-1940 period, but there is a higher proportion of increasing trends in WD and LMR (Fig. 3). Map of the significant ($p < 0.1$) trends manifests a noticeable regional distinction, in which most of the pre-1940 rising trends concentrated over central and north India have turned out to be neutral or decreasing trends during 1961–2004 (Fig. 4). This spatial predominance rainfall increasing trends during 1901–1940 is reflected through the identification of a statistically significant ($p < 0.1$) regional trend (Z_r) after accounting their spatial correlations in PRCPTOT, WD, LMR over the CNI sector only. In particular, significant rise in LMR appears to have contributed to the rise of 39.75 mm decade^{-1} in PRCPTOT (Table 2). From the post-1960 frequency distribution in Fig. 3, it is clear that most parts of the country (i.e., about 70% of 306 grid points) have experienced a drying tendency in wet days (WD) and low-to-moderate rainfall events (LMR), though the distribution of the significant trends (Fig. 4a and d) are location-specific, without identification of any regionally significant pattern.

In general, LMR, an important basic rainfall index that primarily drive changes in PRCPTOT not only for India but also for the whole Asian continent, has declined over southwest Asia (Yao et al., 2008). From the Indian socioeconomic prospective, LMR events (contribute about 85% of PRCPTOT) sustains the monsoon season agriculture, improves the recharge rates and base flows by increasing the opportunity time, and also ensures security of engineering structures in comparison to that of the extreme events. Between the pre-1940 and the post-1960 periods, a clear signal of transition in WD and LMR does not commensurate with the changes in PRECPTOT, particularly in the frequency and spatial consistency of trends during 1961–2004 (Figs. 3–4). This raises the question if the extreme matrices have also undergone any perceptible change, as explored in the following sections.

4.2. Trends in wet and dry spells

Consistent with the wet day (WD) pattern, it is worth noticing that the average longest wet spells, measured through the consecutive wet day (CWD) index, have increased (decreased) during the pre-1940 (post-1960) period, particularly over CNI and NWI, comprising the northern parts of the country (Fig. 2a). Regionally averaged time series show significant downward trend in CWD for all the four domains and the whole country during the post-1960 period (Table 2). This reversal of trend evolution, from a wetting spell to that of a drying spell between the first and later phase of the last century, is more evident from the frequency distribution in Fig. 3 as well as the widespread spatial coverage of the significant trends in Fig. 5; particularly, those post-1960 decreases have a regionally significant trend (Z_r, $p < 0.1$) for all the domains. However, trend analysis over the whole 20th century (1901–2004) appear to have reflected to a large degree the post-1960 drying pattern in WD, LMR and CWD, specifically over central-north India (CNI) and northwest India (NWI), thus offsetting the wetting signals of the pre-1940 period.

More important, however, is to find that the temporal evolution of the 20th century longest dry spells (CDD) does not reflect clearly the signals that we observe using the CWD index, although both the indices are expected to complement each other through opposite signs, as seen during the pre-1940 period (Fig. 3). Particularly, the post-1960 CWD has dropped significantly in grid scale and regional scale, but no clear signal in dry spells (Table 2 and Fig. 3). This type of inconsistency among extreme indices has already been highlighted in the literature (Kiktev et al., 2003; Alexander et al., 2006), and detections of the regional trends here can partly be attributed to the filtering of noises in climatologically heterogeneous settings of India. Interestingly, global scale analysis has displayed a marked decline in the post-1950 globally averaged annual CDD (e.g., Alexander et al., 2006; Donat et al., 2013; Fischer and Knutti, 2014), with a noticeable congregation of the downward trends over central and north India. This contradicts the observed drying trends evident from WD, LMR and CWD over the same region (Fig. 3) and also the previously reported rainfall declines over the core monsoon region (e.g., Bollasina et al., 2011; Singh et al., 2014). Moreover, comparing different HadEX datasets, Donat et al. (2013) show a neutral pattern in CWD during 1951–2003.

Table 2
All India and regional trends (per decade) in the unsmoothed time series of the monsoon rainfall indices.

Indices	Period	All India (AI)	Central-north-India (CNI)	Northwest India (NWI)	Southwest India (SWI)	Southeast India (SEI)	Core monsoon region[a]
PRCPTOT	1901–1940	**23.98**	**39.75**	5.14	21.36	−5.92	**39.05**
	1961–2004	−11.89	−4.80	−9.25	**−45.98**	−5.98	−12.81
	1901–2004	0.10	−3.30	−0.20	0.12	3.05	−1.04
WD	1901–1940	1.01	**1.60**#	−0.21	1.13	−0.74	1.07
	1961–2004	−0.53	−1.03	−1.01	−1.04	−1.24	−0.92
	1901–2004	−0.10	−0.25	−0.18	−0.04	−0.03	−0.14
SDII	1901–1940	0.13	**0.24**	−0.03	0.13	0.07	**0.31**
	1961–2004	0.03	0.09	0.11	**−0.32**#	0.17	−0.03
	1901–2004	**0.05**	0.02	0.06	0.03	**0.09**	**0.06**
LMR	1901–1940	0.77	**1.04**#	0.12	1.00	−0.36	0.89
	1961–2004	−0.55	−0.77	−0.64	**−1.38**	**−0.68**#	−0.89
	1901–2004	−0.08	−0.15	−0.04	−0.05	0.09	−0.02
CDD	1901–1940	−0.34	−0.55	0.26	−0.40	0.08	−0.44
	1961–2004	0.14	0.04	0.42	0.23	**0.85**#	0.00
	1901–2004	−0.04	0.03	−0.08	0.06	0.11	−0.02
CWD	1901–1940	0.22	0.49	0.00	0.82	−0.09	0.32
	1961–2004	**−0.38**	**−0.93**	**−0.37**	**−1.28**	**−0.37**	**−0.78**
	1901–2004	**−0.13**	**−0.26**	**−0.13**	−0.19	0.04	**−0.20**
R70	1901–1940	**0.06**	**0.14**	−0.01	0.05	0.00	**0.10**
	1961–2004	0.01	0.05	0.00	−0.15	0.03	0.01
	1901–2004	**0.02**	0.01	0.00	0.01	0.01	−0.01
R100	1901–1940	**0.03**	**0.06**	−0.01	0.03	0.00	**0.04**#
	1961–2004	0.01	**0.04**#	0.00	−0.03	0.00	0.02
	1901–2004	**0.01**	0.00	0.00	0.00	**0.01**	0.005
R150	1901–1940	**0.01**	**0.02**	0.00	0.00	0.00	0.01
	1961–2004	0.008	0.007	0.00	0.008	0.00	**0.01**
	1901–2004	**0.007**	**0.003**	0.00	0.00	0.00	**0.004**
Rx1day	1901–1940	**1.08**#	0.91	0.34	−1.75	1.40	1.12
	1961–2004	1.13	**2.27**#	0.96	−0.72	−2.56	**2.55**#
	1901–2004	**0.40**	**0.78**	**0.94**	−0.28	−0.44	**0.84**
Rx5day	1901–1940	2.39	3.44	−0.61	−0.38	2.48	2.23
	1961–2004	0.66	1.69	1.27	−3.53	**−4.97**	2.10
	1901–2004	0.11	0.71	1.15	−0.03	**−1.36**#	1.14
R95p	1901–1940	4.34	**20.70**	−0.43	5.45	−0.16	**16.30**
	1961–2004	6.19	6.19	1.34	−6.51	5.02	2.82
	1901–2004	**1.84**#	−0.14	0.81	1.60	**2.03**#	1.44
R99p	1901–1940	−0.21	**9.49**	−0.37	0.97	1.23	4.97
	1961–2004	**8.65**	**6.06**	2.85	1.85	**3.94**	**4.98**
	1901–2004	**1.35**	0.47	0.65	0.22	**1.11**	0.88
R95pTOT	1901–1940	−0.08	**0.79**#	0.10	0.43	0.53	**0.84**#
	1961–2004	**0.59**	0.39	0.91	−0.10	1.15	0.33
	1901–2004	**0.14**#	0.00	0.24	−0.02	0.26	0.11
R99pTOT	1901–1940	−0.21	**0.47**#	−0.25	0.23	0.27	0.31
	1961–2004	**0.55**	0.23	0.44	0.27	**0.59**#	**0.42**
	1901–2004	**0.08**#	0.04	0.04	−0.05	0.11	0.06

Bold and bold with # values correspond to the trends significant at the 5% and 10% levels, respectively (i.e., $p < 0.05$ and 0.1).
[a] Core monsoon region (18°–28° N, 73°–82° E).

It is, therefore, important to discuss whether the CDD index is relevant enough to assess the dry spells of the monsoon season, or the CWD index is more informative, given their sensitivity to the dichotomy of rainfall distribution within the season. In fact, there is a likelihood that the longest wet spell (CWD) could occur in the rainiest month of July and/or August (both the months contribute about 62% of PREPTOT), while the longest dry spell (CDD) could be in the relatively dryer months of June or September. While there is strong agreement in the frequency and spatial locations of significant trends between the pre-1940 CDD and CWD shown in Figs. 3 and 5, the contradiction of the post-1960 period can be rooted to the recent non-uniform rainfall distribution. A part of the post-1960 decreases in dry spells could be a manifestation of the increased wetness of June rather than the drying tendency from July to September. Monthly analysis of CDD and CWD provides reasonable explanation to such presumption, as the nationally averaged June CDD has exhibited a significant downward trend during 1961–2004 (also complemented by a significant rise in CWD), but contradicts the nonsignificant increases in other months of the monsoon season. This finding is also corroborated by the grid scale results, with the dry spell (CDD) declines in 74% of the geographical area in June, whereas the rest of the monsoon months indicate increases over 55% of grid points. For CWD, a decreasing tendency is observed in about 66% of the grid points during July to September, similar to the whole monsoon scale results (Fig. 3), while an opposite tendency with similar proportions is seen in June.

Consistently, several previous researches have pointed out this dichotomy within the monsoon season, a wetting June and a drying July to September months (e.g. Gautam et al., 2009; Lau and Kim, 2010; Panda and Kumar, 2014). Thus, it appears logical to infer that the CWD index is pertinent to capture the observed drying patterns of the recent decades. Moreover, agricultural droughts during the critical growth stages of the monsoon rain-dependent crops, for example in 2000 and 2002 causing significant socioeconomic crisis in India (Gadgil and Gadgil, 2006), is mainly due to a drop in WD and CWD in July and August.

4.3. Trends in extreme indices

Noteworthy feature of the 20th century monsoon climate is the conspicuous rise in the frequency and intensity of the extreme rainfall indices during the post-1960 period, as depicted in the nationally averaged smoothed time series of the wet extremes (e.g., SDII, R100, Rx1day, and R95pTOT) (Fig. 2a). Nationally, an initial low-frequency and below-average oscillation can be seen before a high frequency rise

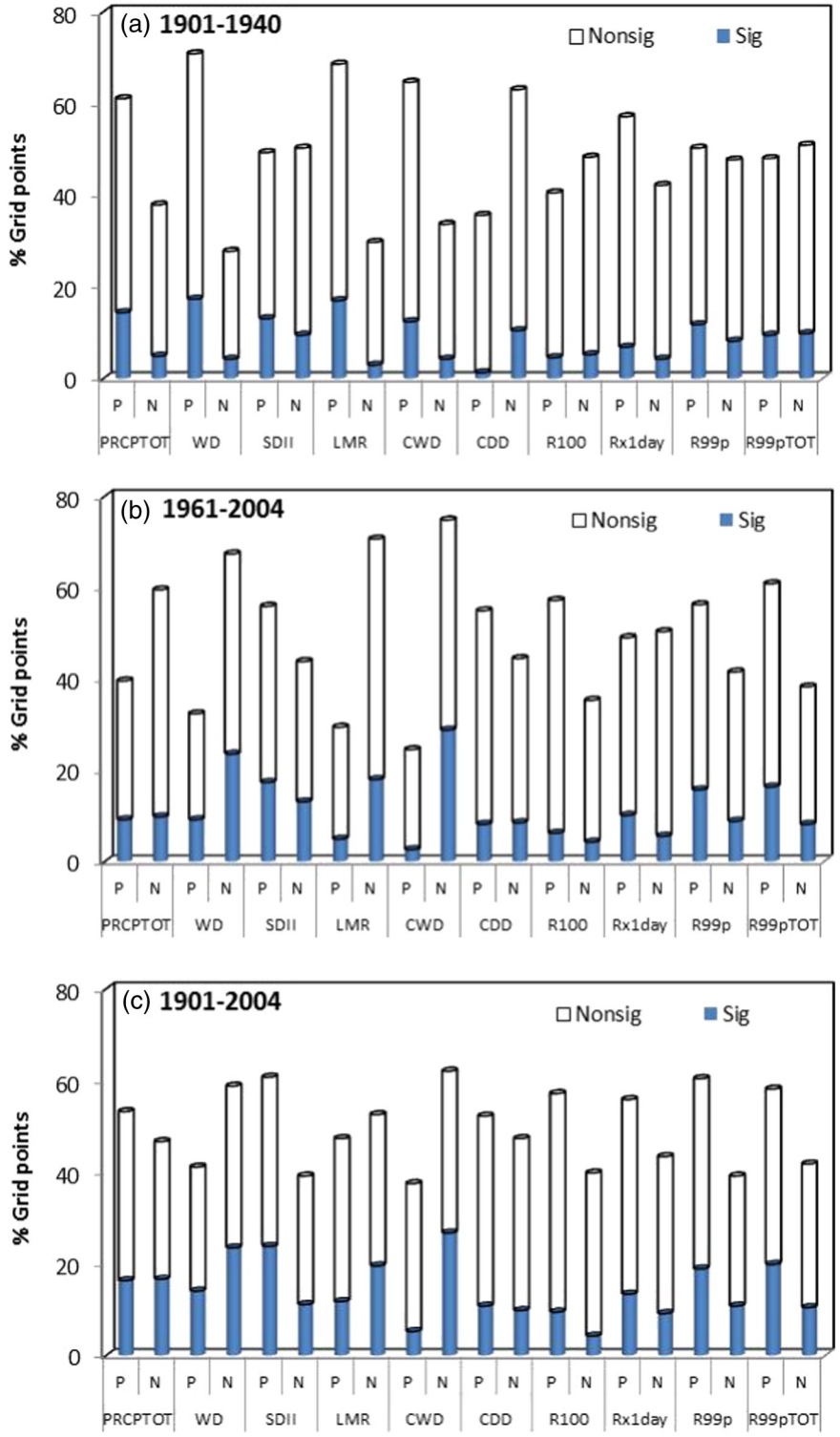

Fig. 3. Comparison of the percentage of 306 grid points with positive (P) and negative (N) trends along with the percentage of their significant ($p < 0.1$) trends (shaded) in the basic and extreme monsoon rainfall indices (Table 1) during the (a) 1901–1940, (b) 1961–2004 and (c) 1901–2004 period.

since the 1970s. However, the patterns over central-north India (CNI), where most of the extreme events generally occur, stand out clear in terms of two sharp rises, one each during the first and last decades of the study period. Although identification of grid scale trends in extreme matrices (Fig. 3) is naturally difficult, spatial averaging, as suggested by Goswami et al. (2006), appears to have yielded significant trends for some indices over CNI and all India (Table 2). However, it is important to note how the level of spatial aggregation and definition of extremes have yielded different results, which has led to disagreement over the spatiotemporal evolution in the recent studies (e.g., Ghosh et al., 2012). For example, analysing the south Asian summer rainfall, Yao et al. (2008) reported a downward trend in extreme and heavy rainfall

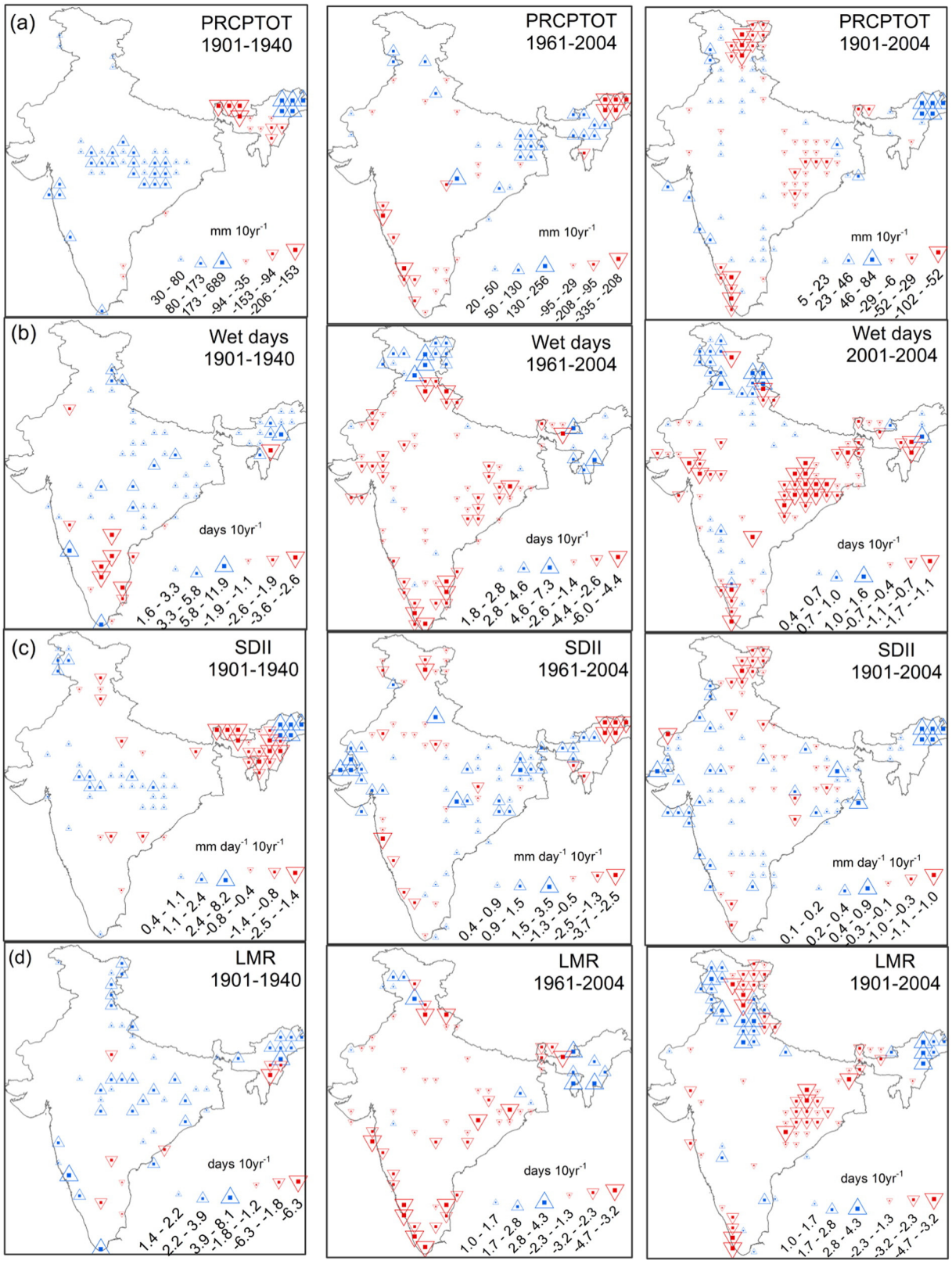

Fig. 4. The spatial map of the significant ($p < 0.1$) trends in (a) PRCPTOT, (b) wet days, (c) SDII and (d) LMR during 1901–1940, 1961–2004, and 1901–2004. Blue triangles show the increasing trends and red inverted triangles show the decreasing trends, with the sizes of the triangles proportionate to the rate of change (i.e. Kendall slope) per decade. (For interpretation of the references to colour in this figure legend, the reader is referred to the web version of this article.)

during 1979–2002 over India using the index R50, contradicting our findings in R70 (Table 2). This means that R50 has reflected a large part of the LMR events, which is not captured in R70.

From the frequency distribution of the grid scale results in Fig. 3, the significant increasing trends are more often detected during the 1961–2004 and 1901–2004 periods in the percentile-based rainfall intensity

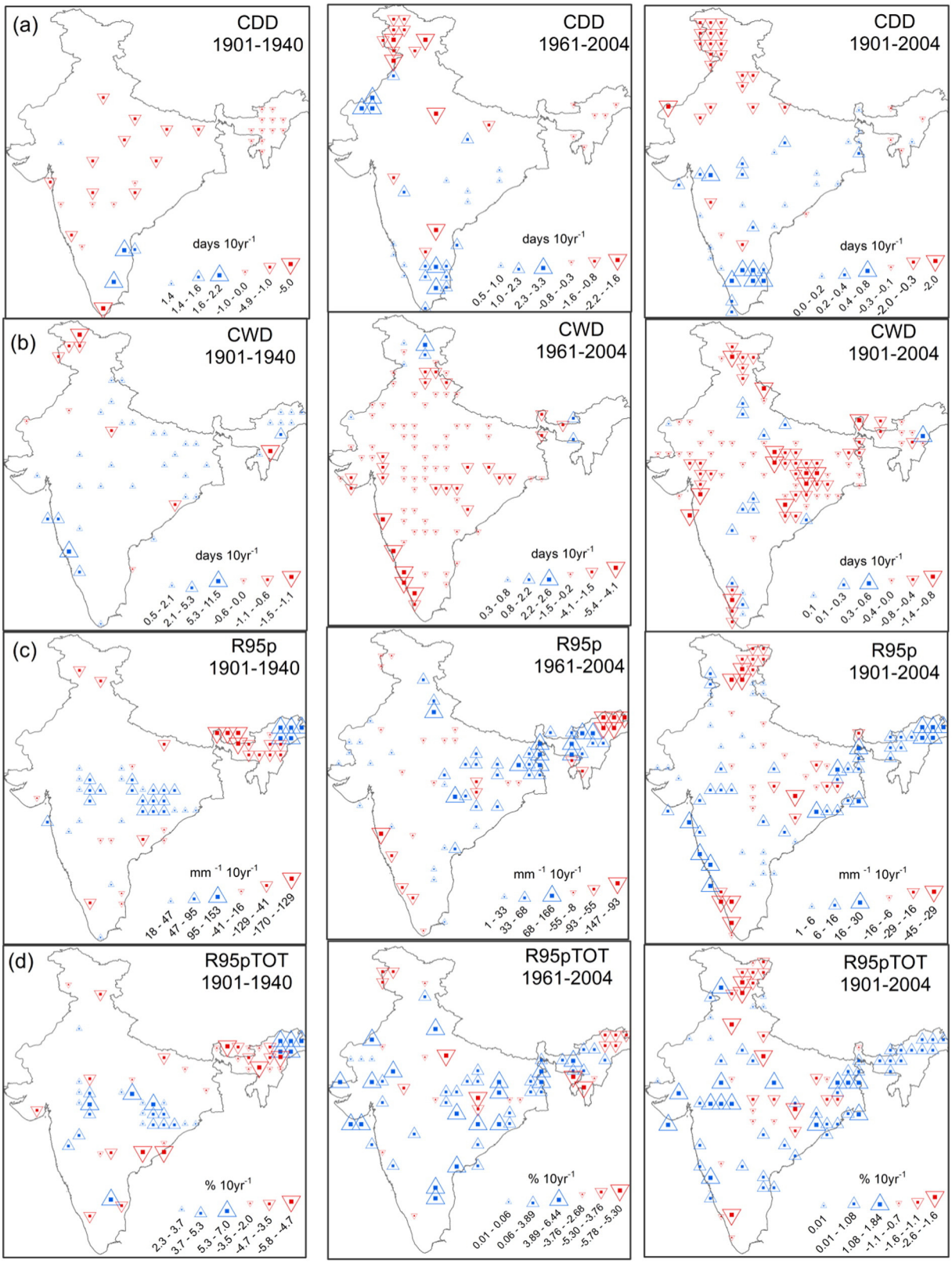

Fig. 5. Same as Fig. 4, but for (a) CDD, (b) CWD, (c) R95p and (d) R95pTOT.

indices (R95p, R99p, R95pTOT and R99pTOT), which are importance for the global climate change assessment and comparisons. Their spatial occurrence (Figs. 4–6) indicates that the stronger upward trends, particularly in contribution from very and extreme wet days, R95pTOT and R99pTOT (Fig. 5d), have a larger geographic coverage. A similar spatial distribution of the significant trends of average wet day rainfall intensity index (i.e., SDII) and wet day frequency (WD) shown in Fig. 4b and c suggests that the increases in SDII could be due to the decreases in WD. However, a significant rise in R95pTOT and R99pTOT, which are insensitive to WD, explains that both these episodes of decreases in

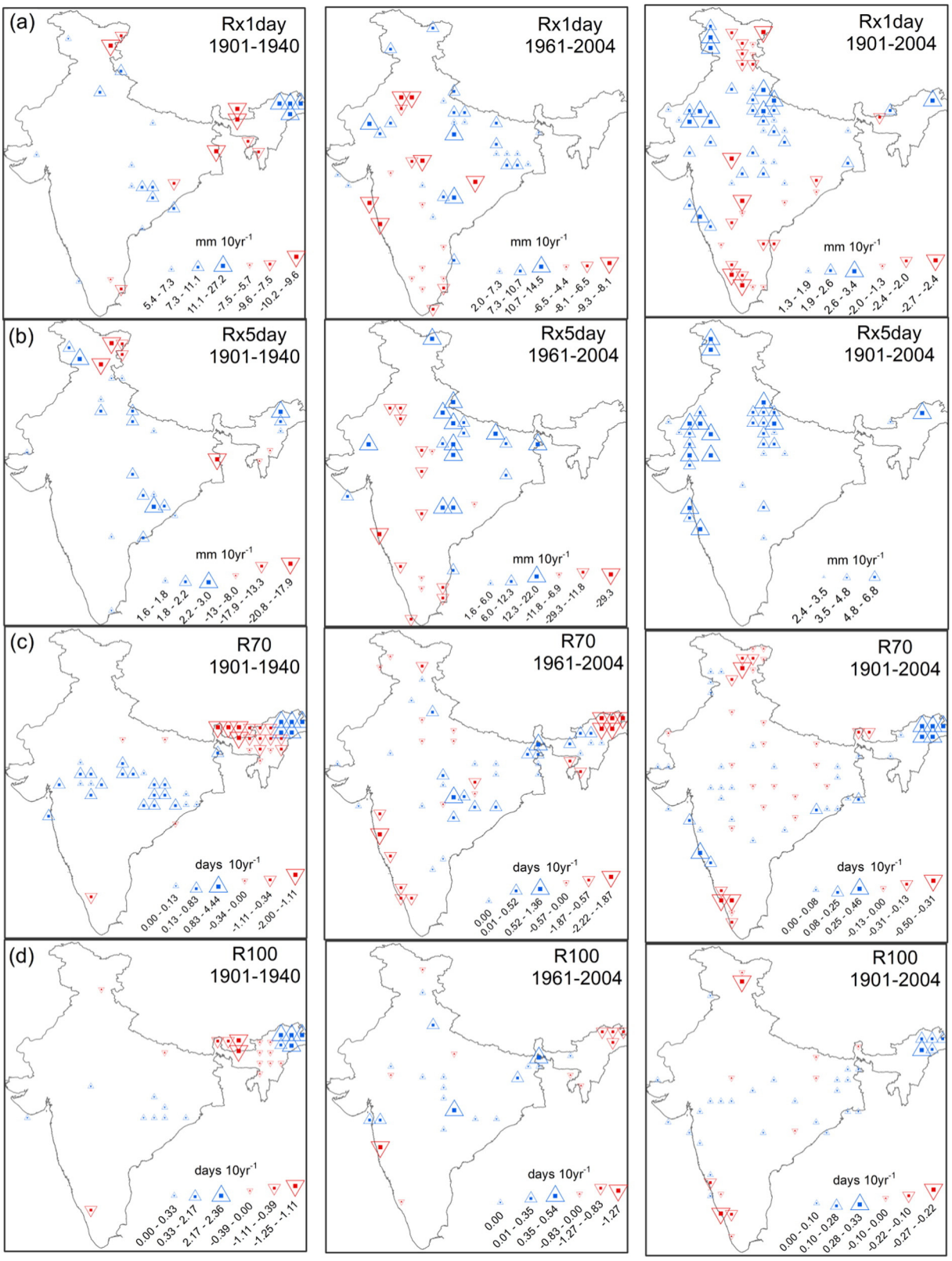

Fig. 6. Same as Fig. 4, but for (a) Rx1day, (b) Rx5day, (c) R70, and (d) R100.

WD and increases in extreme events have co-occurred. A spatially less regular pattern is observed in the threshold-based frequency of heavy rainfall events, R70 and R100 (Fig. 6c and d), because these are local events confined to certain parts of central, northeast and southwest India only. Similarly, although Rx1day and Rx5day are spatially representative indices of absolute rainfall intensity, they only capture a part of the entire monsoon period with a high year-to-year variability. Although the spatial outlines of the core monsoon and CNI regions are

slightly different, R99p and R99pTOT have a regionally significant trend (Z_r) over the core monsoon region, while Rx1day is significant over CNI during the post-1960 period.

Nevertheless, use of a high resolution gridded dataset has allowed us to identify the patches where the indices with potential threat to human and infrastructure have increased significantly in the post-1960 period. In particular, irrespective of the indices, parts of the central and north-west India appear to be more vulnerable, where most of the upward trends of high magnitudes have congregated (Figs. 4–6). These results are consistent with the findings of Vittal et al. (2013) who used the same dataset but a different methodology on percentile-based measures of rainfall extremes. The 20th century (1901–2004) changes are likely to be driven by the trends during 1961–2004 for most of the indices. From the spatial distribution of the 1901–2004 period trends, however, it appears that the large-scale pre-1940 rising patterns in WD and LMR have been masked by that of the post-1960 period trends, while a part of the pre-1940 increases in PRCPTOT is retained, possibly due to the cancellation of the observed dry and wet extremes during 1961–2004. Moreover, with the increasing wet extremes during 1961–2004, the observed decreases in wet days can be attributed to the declining LMR frequency. In general, statistical detection of trends in extreme rainfall indices remains challenging due to its nonlinearity and its very local nature of occurrence (Groisman et al., 2005), and this could be the primary reason for the spatially less consistent patterns observed in

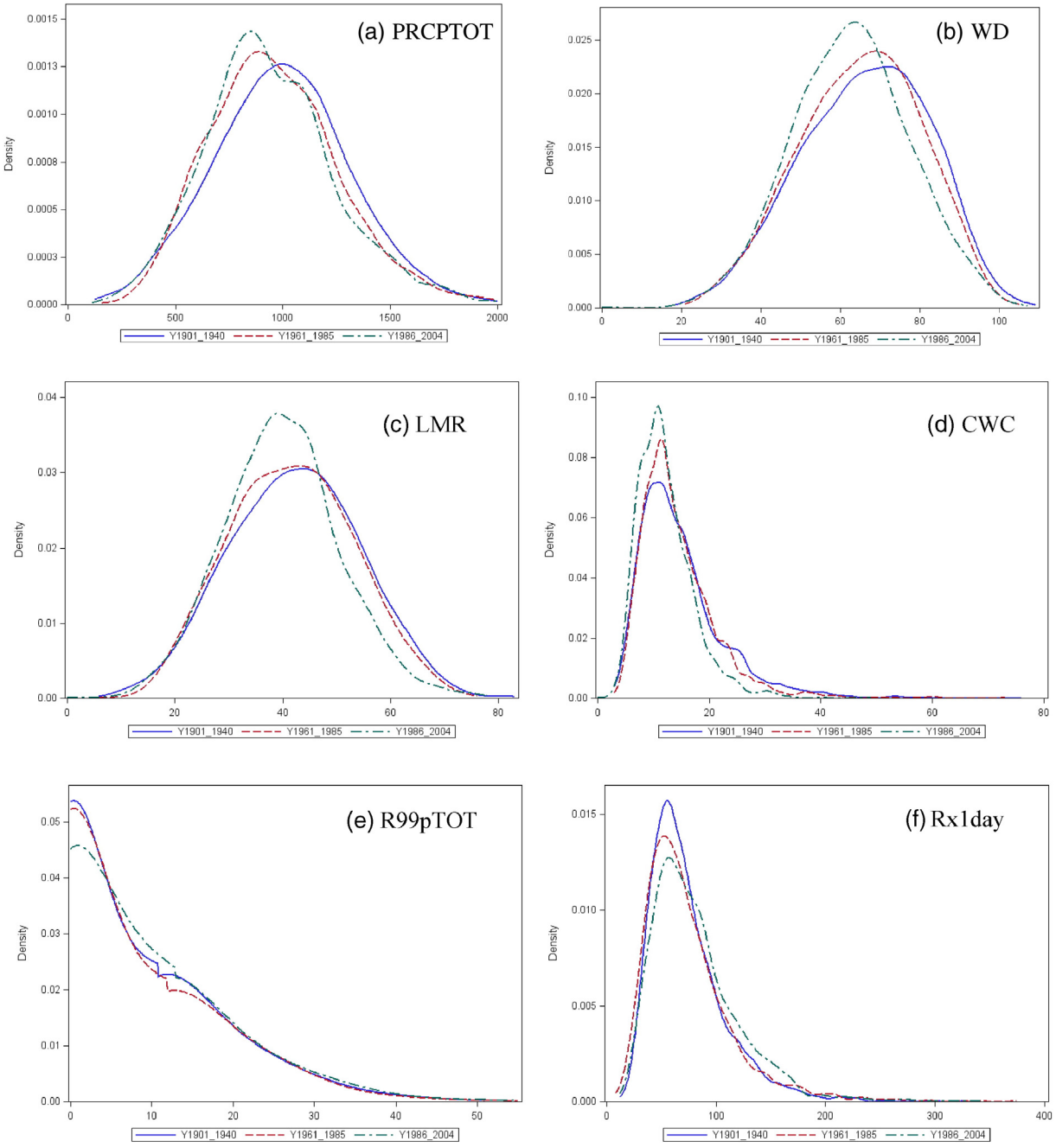

Fig. 7. Probability density functions (PDFs) of some selected monsoon rainfall indices (a to f) during the 1901–1940 (pre-1940, blue continuous line), 1961–1985 (pre-1985, discrete line) and 1986–2010 (post-1985, discrete with dot line) periods. (For interpretation of the references to colour in this figure legend, the reader is referred to the web version of this article.)

this study and also in other parts of the world during the second half of the 20th century (e.g., Zolina et al., 2008; Donat et al., 2013; Fischer and Knutti, 2014).

4.4. Changes in probability density function (PDF)

Fig. 7 illustrates the spatiotemporal changes within the second half of the 20th century and departure from that of the first half through the probability density function (PDF) during the 1901–1940 (pre-1940), 1961–1985 (pre-1985) and 1986–2010 (post-1985) periods from the grid scale monsoon rainfall indices over central-north India (CNI), which has been highlighted in the literature because of its climatic evolutions (Bollasina et al., 2011; Singh et al., 2014). Note that, in the first 40 years (pre-1940), the PDFs of the basic rainfall indices (PRCPTOT, WD and LMR) resemblances a normal distribution, but in the later periods (i.e., pre-and post-1985) a clear asymmetry is evident with a change towards the dryer part. For PECPTOT, changes in the mean between the former (pre-1940) and later periods are statistically significant ($p < 0.05$), but not the changes in variance. For WD and LMR, however, both the mean and variance have changed significantly among the sub-periods; similar is also the changes in the PDFs of CWD (Fig. 7d). In extreme indices, the change in Rx1day is more noticeable compared to R99pTOT (Fig. 7e and f), with the recent period displaying a significant rise in the mean Rx1day over that of the pre-1940 and pre-1960 periods. Moreover, Rx1day is also characterized by a significant change in variance. These changes are in agreement with the expected shifts from the normal to weak and strong monsoons (i.e., change in tails of the PDFs) in a warmer climate (Turner and Annamalai, 2012).

4.5. Trends in palmer drought severity index (PDSI)

To draw further insights into the drying monsoon climate of recent decades in India, we use the Palmer Drought Severity Index (PDSI), which has been used widely as a meteorological drought index (Dai, 2011). Fig. 8 illustrates the monsoon season spatial average and variance of the monthly PDSI index over all India (AI) and central-north India (CNI) during 1961–2010. The observed high interannual variability of the average PDSI is consistent with the rainfall (PRCPTOT) variability, with a significant ($p < 0.05$) correlation coefficient of 0.86 and 0.77 for AI and CNI, respectively during the common period 1961–2004. Occurrence of both the negative (dry) and positive (wet) anomalies, with some century scale extreme droughts since 2000, has resulted in a nonsignificant drying trend in the mean PDSI of the AI and CNI time series. A significant rise in the spatial variance of PDSI, with marked increases since the mid-1980s (Fig. 8), is indicative of the lack of uniform pattern of both dry and wet conditions, as highlighted by Ghosh et al. (2012) and Singh et al. (2014). This increased spatial variability in PDSI is consistent with the post-1985 period increased mean and variances of the extreme rainfall indices over CNI (Fig. 7).

We, therefore, compare the pre-1985 (1961–1985) and post-1985 (1986–2010) period PDFs of all India (AI) and central-north India (CNI) monthly PDSI index to detect if such non-stationarity exists (Fig. 9). From the national distribution, signal of an increased occurrence of both dry and wet extremes is evident from the raised opposite PDF tails, with a higher frequency of the post-1985 extreme droughts. In general, a change in the tails of the PDF is more important from climate change impacts and risk assessment prospective rather than the mean. However, the major mode of the PDF (i.e., peak), which corresponds to the negative anomalies, suggests the prevalence of a drying condition during the whole 1961–2010 period (Fig. 9),

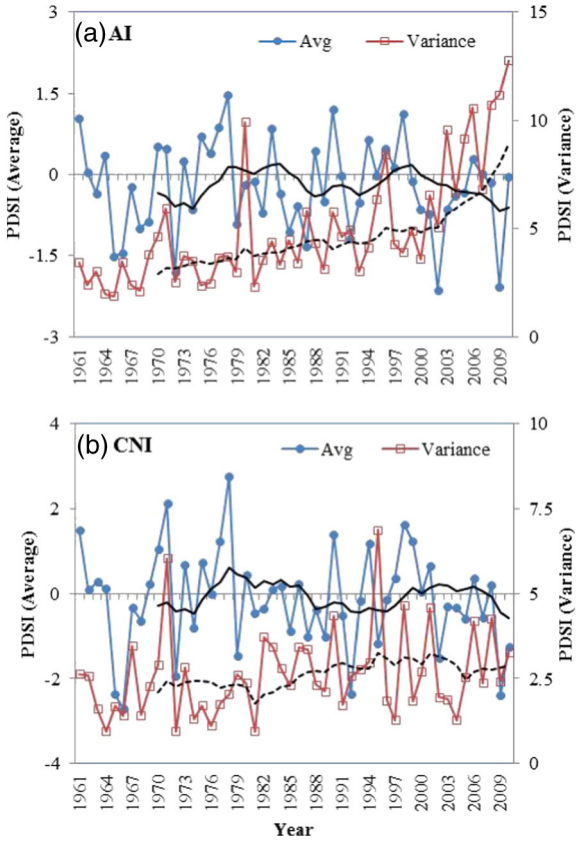

Fig. 8. Time series of the monsoon season spatial average and variance of monthly PDSI for (a) all India (AI) and (b) central-north India (CNI) during 1961–2010, along with their 10-year running mean (bold line for the average and discrete line for the variance).

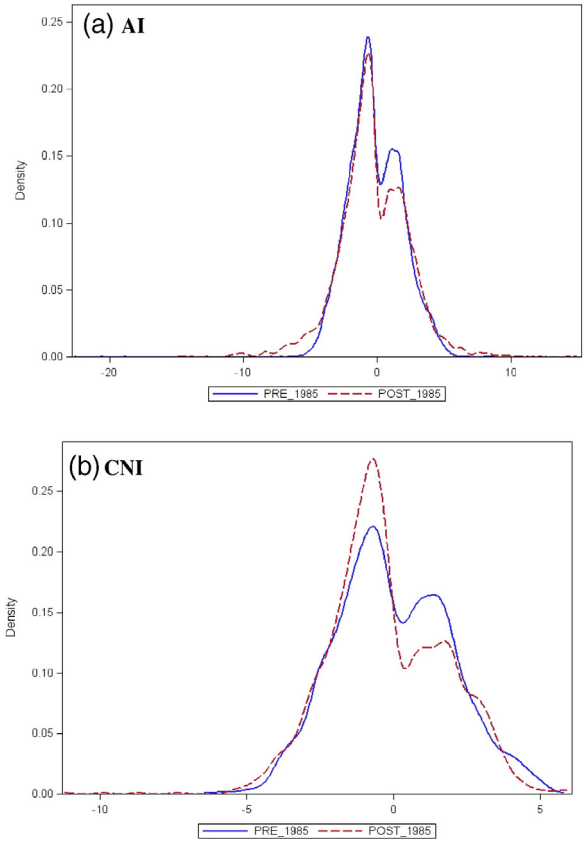

Fig. 9. Probability density function (PDF) of the pre-1985 (1961–1985, continuous line) and the post-1985 (1986–2010, discrete line) period: (a) all India (AI) and (b) central-north India (CNI) monthly PDSI.

thereby lending support to the widely reported weakening of the monsoon circulation.

In particular, the spatially prominent drying patterns in the central and north-central parts discussed in the previous section are clearly reflected in its PDSI, with a negatively skewed PDF (elongated left tail) and negative modes (Fig. 9b). Results of the global scale PDSI analysis have also indicated a drying trend over the northern parts of India, as an integral part of a general rise in aridity in south Asia since 1950 (Dai, 2011). Moreover, for the adjacent country China, Sun et al. (2016) observed more drying trends in the Loess Plateau during 1986–2013 compared to that of 1960–1985 due to a weaker eastern Asian summer monsoon. Nevertheless, it can be seen that the frequency and intensity of droughts in India have increased in recent years, particularly the occurrence of century scale droughts in 2002 and 2009, leading to changes in the mean PDSI state over CNI, as the post-1985 PDF indicates a slight negative shift along with a noticeable rise in the PDF peak (Fig. 9b); in particular, the 2009 drought effect, as reflected in terms of an anomalous PDSI value (Fig. 8b), also led to pronounced terrestrial water storage (TWS) losses in the groundwater-irrigated northern and central parts of India (Panda and Wahr, 2016). Consistently, Singh et al. (2014) observed more decreases in the mean rainfall and wet spell frequency in the core monsoon belt covering a major portion of CNI during 1981–2011 compared to that of the period 1951–1980. For the all India (AI) PDSI values shown in Fig. 9a, a change in the upper and lower tail of the PDF with no clear difference in the mean suggests the increased occurrence of opposite extremes.

4.6. Linkages with SST

Identification of the causes of the trends and variability of the monsoon rainfall of India remains an active area of research because of the complex interaction between the Ocean and the landmass. In particular, a strong warming of the adjacent tropical Indian Ocean sea surface temperature (TIO SST) and also that of the remote NINO3.4 region (Fig. 2b) have been reported to have influenced the Asian monsoon in general. Even in absence of a strong El Niño (NINO3.4) condition, the major drought years of 2000 and 2002 have been attributed to the rise in SST over the equatorial Indian Ocean, which induced intense monsoon breaks through modulating the strength of the monsoon Hadley circulation (Krishnan et al., 2006). However, correlation analysis indicates that the basic and extreme matrices of the monsoon rainfall, which have undergone non-linear to multidecadal changes, exhibiting no direct correspondence on a year-to-year basis with the TIO SST and NINO3.4 indices during 1901–2004 (Fig. 2a and b), except partially for R100 ($r = 0.30$, $p < 0.05$) and R150 ($r = 0.40$, $p < 0.05$) with TIO SST. But removal of the decadal variability through smoothing the TIO SST time series with a 10-year running mean, as followed by Rajeevan et al. (2008), led to an improvement of the linear relationship with R100 ($r = 0.71$) and R150 ($r = 0.83$); moreover, a significant inverse relationship is observed with WD, LMR and CWD in contrast to a significant positive relationship with most of the wet extremes.

While the smoothed pre-1940 time series of all the considered rainfall indices reflect a relatively high degree of positive (negative for CWD) correspondence with the TIO SST anomalies (average r of 0.62), a transition in the sign of correlation is observed during the post-1960 period for PRCPTOT, WD, LMR and CWD, with an average r of −0.32. Important to note that the TIO SST (Fig. 2b) has experienced a stronger warming rate of 0.12 °C decade^{-1} during 1961–2004 in comparison to 0.07 °C decade^{-1} during 1901–1940, while a cooling trend (i.e., −0.11 °C decade^{-1}) is observed during 1941–1960. In the background of a little warming of the land surface temperature during 1901–1940, with Tmax (daytime) experiencing a nonsignificant trend of 0.03 °C decade^{-1} and Tmin (night) a neutral trend, the pre-1940 rainfall changes is likely to be associated with the increasing tropical depression frequency (i.e., 0.45 decade^{-1}) that generally form over the Bay of Bengal and propagate northwestward into the monsoon trough, contributing to the mean and extreme rainfalls over CNI. In addition to the ocean warming, both Tmax and Tmin have shown a pronounced warming rate of 0.11 and 0.13 °C decade^{-1}, respectively during the post-1960 period, a period during which most of the conflicting trend results have been reported.

It is therefore important to find the extent to which the observed grid scale trends co-vary with the TIO SST and NINO3.4 indices during 1961–2004. The PMK test results show that the strength of the trends are better modulated by the TIO SST index with a notable decrease in the proportion of significant ($p = 0.1$) trends (Fig. 10). Its comparison with the results obtained from the original time series (Fig. 3b), about 2% and 6% grids are found to be significantly increasing and decreasing, respectively for PRCPTOT after accounting the TIO SST index, corresponding to an equal proportion of 10% grids in the original time series. For wet days and LMR, the proportion of significant negative trends has dropped from >20% of grids in the original time series (Fig. 3b) to an average of 10% and 14% with the association of the TIO SST and NINO3.4 indices, respectively. However, the TIO SST index accounts for a large part of the wet spell (CWD) trends with the identification of significant decreasing trends in 11% of grids only, which is about two-and-half time less than the proportion observed in the original time

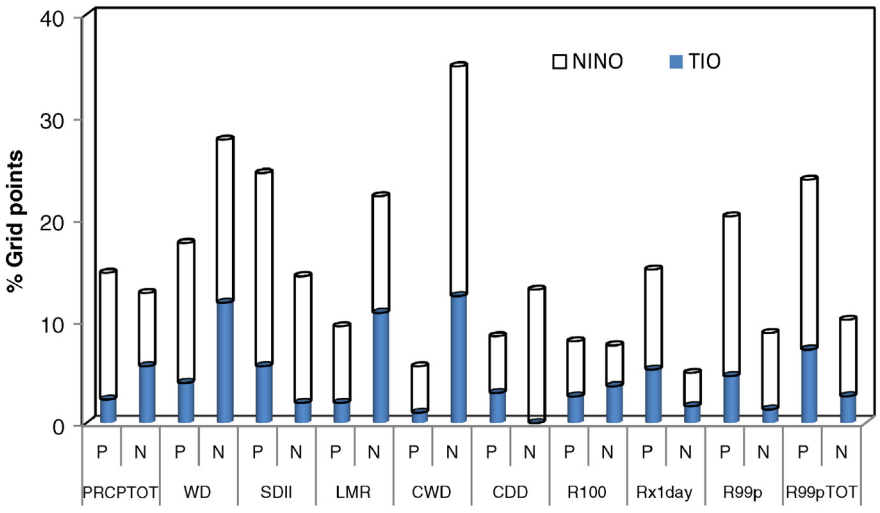

Fig. 10. Percentage of 306 grid points with significant ($p < 0.1$) positive (P) and negative (N) trends in the basic and extreme monsoon rainfall indices after accounting the TIO SST and NINO3.4 indices (shaded differently) through the PMK test during 1961–2004.

series (Fig. 3b), but for the NINO3.4 index it is 23% of grids. Other notable changes include the drop in the significant upward trend proportions from 10% to 3.6% in Rx1day, 6% to 2.6% in R100, 15.6% to 5.5% in R99p, and 16.3% to 7.9% in R99pTOT after removing the influence of the TIO SST index (Fig. 10). Interestingly, the observed influence of the TIO SST index assessed through the PMK test has been found to be robust, as we also obtained similar proportion of significant trends using the method followed by Vincent et al. (2015).

In general, the post-1950 weakening of the southwest summer monsoon flow through the increased frequency and duration of monsoon break phases has been attributed to the SST warming over the tropical eastern IO (Ramesh Kumar et al., 2009). Note that the CWD index reflects rainfall in a single spell of days compared to other indices, typically representing the active phase of the monsoon rainfall. The increased sensitivity of CWD to the TIO SST index therefore supports the reported frequent monsoon breaks due to warming of the adjacent Ocean, which has led to more occurrences of drying tendencies. Moreover, the observed significant drop in the depression frequency (i.e., -0.60 decade^{-1}) supports the widely reported weakening of the monsoon circulation. Although some of the extreme features of the monsoon rainfall are showing similar responses to what has been reported as an expected outcome of the anthropogenic warming (Giorgi et al., 2011; Westra et al., 2013; Zhang et al., 2013), the observed spatial inconsistency could be due to local factors, such as urbanization, land-use change and orography. A large number of driving factors appear to have contributed to the extremes of varying nature and extent observed in this study, thus posing a challenge to the validation and attribution studies.

5. Conclusions

This study presents the 20th century (1901–2004) changes in the mean and extreme monsoon rainfall indices, developed by the ETCCDI, of India using robust statistical tools. Nationally and regionally averaged anomalies show multidecadal variability with marked differences, suggesting the fact that the country-wide time series does not depict the spatial diversity of the monsoon rainfall. Comparison of the rainfall matrices between the pre-1940 and post-1960 periods exhibits a noteworthy transition from a wetting condition to a drying tendency, particularly in PRCPTOT, WD, LMR and CWD of central-north India (CNI). Moreover, the probability density function (PDF) of rainfall and PDSI indices indicate a significant change in the spatiotemporal variability during the post-1985 period. The first decade of the 21st century (i.e., 2001–2010) has witnessed the worst droughts since the beginning of the 20th century in the years 2002 and 2009, along with the regionally devastating floods of 2005 and 2008, leading to drop in food grain production of about 10%. These events appear to be highly unlikely without the role of the post-1960 trends, though the fundamental natural variability of the monsoon rainfall cannot be understated. If such opposite extremes continue in the future, generally anticipated in a warmer climate, the spatial variability would rise but not detectability of trends, as reflected in the PDSI index.

Compared to the recently reported global scale identification of significant trends in extreme indices, we find a less proportion of significant trends, with some indices even displaying a contradictory tendency. This, in general, underscores the importance of the season of analysis and the choice of the extreme indices, particularly for the highly heterogeneous monsoon climate of India. Although warming of the TIO SST index explains a degree of association, a detailed attribution, which is beyond the scope of this study, will enhance the understanding in the context of the reported multiple drivers of the monsoon rainfall changes. Given the vulnerability of India to the impending water and food crisis, the results of the current study can be used as a reference to implement the location-specific adaptation and mitigation measures.

Acknowledgements

Grant of the Indian Council of Agricultural Research (ICAR), New Delhi to undertake this research is duly acknowledged. We thank the anonymous reviewers for their comments and suggestion to improve the contents of this paper.

References

Alexander, L.V., Zhang, X., Peterson, T.C., Caesar, J., Gleason, B., Klein Tank, A.M.G., Haylock, M., Collins, D., Trewin, B., Rahimzdeh, F., Tagipour, A., Kumar, K.R., Revadekar, J.V., Griffiths, G., Vincent, L., Stephenson, D.B., Burn, J., Aguilar, E., Brunet, M., Taylor, M., New, M., Zhai, P., Rusticucci, M., Vazquez, A.J.L., 2006. Global observed changes in daily climate extremes of temperature and precipitation. J. Geophys. Res. 111, D05109. http://dx.doi.org/10.1029/2005JD006290.

Ali, H., Mishra, V., Pai, D.S., 2014. Observed and projected urban extreme rainfall events in India. J. Geophys. Res. 119. http://dx.doi.org/10.1002/2014JD022264.

Bollasina, M.A., Ming, Y., Ramaswamy, V., 2011. Anthropogenic aerosols and the weakening of the South Asian summer monsoon. Science 334, 502–505.

Brunetti, M., Maugeri, M., Monti, F., Nanni, T., 2004. Changes in daily precipitation frequency and distribution in Italy over the last 120 years. J. Geophys. Res. 109, D05102. http://dx.doi.org/10.1029/2003JD004296.

Dai, A., 2011. Characteristics and trends in various forms of the palmer drought severity index (PDSI) during 1900–2008. J. Geophys. Res. 116, D12115. http://dx.doi.org/10.1029/2010JD015541.

Dai, A., Trenberth, E., Qian, T., 2004. A global data set of palmer drought severity index for 1870–2002: relationship with soil moisture and effects of surface warming. J. Hydrometeorol. 5, 1117–1130.

Dash, S.K., Kulkarni, M.A., Mohanty, U.C., Prasad, K., 2009. Changes in the characteristics of rain events in India. J. Geophys. Res. 114, D10109. http://dx.doi.org/10.1029/2008JD010572.

De Luis, M., Gonzalez-Hidalgo, J.C., Longares, L.A., Stepanek, P., 2009. Seasonal precipitation trends in the Mediterranean Iberian peninsula in second half of 20th century. Int. J. Climatol. 29, 1312–1323.

Donat, M.G., Alexander, L.V., Yang, H., Durre, I., Vose, R., Dunn, R.J.H., Willett, K.M., Aguilar, E., Brunet, M., Caesar, J., Hewitson, B., Jack, C., Klein Tank, A.M.G., Kruger, A.C., Marengo, J., Peterson, T.C., Renom, M., Oria, R.C., Rusticucci, M., Salinger, J., Elrayah, A.S., Sekele, S.S., Srivastava, A.K., Trewin, B., Villarroel, C., Vincent, L.A., Zhai, P., Zhang, X., Kitching, S., 2013. Updated analyses of temperature and precipitation extreme indices since the beginning of the twentieth century: the HadEX2 dataset. J. Geophys. Res. 118, 2098–2118.

Douglas, E.M., Vogel, R.M., Kroll, C.N., 2000. Trends in floods and low flows in the United States: impact of spatial correlation. J. Hydrol. 240 (1–2), 90–105.

Duhan, D., Pandey, A., 2013. Statistical analysis of long term spatial and temporal trends of precipitation during 1901–2002 at Madhya Pradesh, India. Atmos. Res. 122, 136–149.

Fischer, E.M., Knutti, R., 2014. Detection of spatially aggregated changes in temperature and precipitation extremes. Geophys. Res. Lett. 41. http://dx.doi.org/10.1002/2013GL058499.

Gadgil, S., Gadgil, S., 2006. The Indian monsoon, GDP and agriculture. Econ. Polit. Wkly. 41, 4887–4895.

Gallant, A.J.E., Karoly, D.J., 2010. A combined climate extremes index for the Australian region. J. Clim. 23, 6153–6165.

Gallego, M.C., Trigo, R.M., Vaquero, J.M., Brunet, M., García, J.A., Sigró, J., Valente, M.A., 2011. Trends infrequency indices of daily precipitation over the Iberian Peninsula during the last century. J. Geophys. Res. 116, D02109. http://dx.doi.org/10.1029/2010JD014255.

Gautam, R., Hsu, N.C., Lau, K.M., Kafatos, M., 2009. Aerosol and rainfall variability over the Indian monsoon region: distributions, trends and coupling. Ann. Geophys. 27, 3691–3703.

Ghosh, S., Das, D., Kao, S.-C., Ganguly, A.R., 2012. Lack of uniform trends but increasing spatial variability in observed Indian rainfall extremes. Nat. Clim. Chang. 2, 86–91.

Giorgi, F., Im, E.-S., Coppola, E., Diffenbaugh, N.S., Gao, X.J., Mariotti, L., Shi, Y., 2011. Higher hydroclimatic intensity with global warming. J. Clim. 24, 5309–5324.

Goswami, B.N., Venugopal, V., Sengupta, D., Madhusoodanan, M.S., Xavier, P.K., 2006. Increasing trend of extreme rain events over India in a warming environment. Science 314, 1442–1445.

Goyal, M.K., 2014. Statistical analysis of long term trends of rainfall during 1901–2002 at Assam, India. Water Resour. Manag. 28 (6), 1501–1515.

Griffiths, M.L., Bradley, R.S., 2007. Variations of twentieth-century temperature and precipitation extreme indicators in the northeast United States. J. Clim. 20, 5401–5417.

Groisman, P.Y., Knight, R.W., Easterling, D.R., Karl, T.R., Hegerl, G.C., Razuvaev, V.N., 2005. Trends in intense precipitation in the climate record. J. Clim. 18 (9), 1326–1350.

Guhathakurta, P., Rajeevan, M., Sikka, D.R., Tyagi, A., 2015. Observed changes in southwest monsoon rainfall over India during 1901–2011. Int. J. Climatol. 35, 1881–1898.

Hasson, S., Pascale, S., Lucarini, V., Böhner, J., 2016. Seasonal cycle of precipitation over major river basins in South and Southeast Asia: a review of the CMIP5 climate models data for present climate and future climate projections. Atmos. Res. 180, 42–63.

Joshi, M.K., Pandey, A.C., 2011. Trend and spectral analysis of rainfall over India during 1901–2000. J. Geophys. Res. 116, D06104. http://dx.doi.org/10.1029/2010JD014966.

Kenyon, J., Hegerl, G., 2010. Influence of modes of climate variability on global precipitation extremes. J. Clim. 23, 6248–6262.

Kiktev, D., Sexton, D., Alexander, L., Folland, C., 2003. Comparison of modeled and observed trends in indices of daily climate extremes. J. Clim. 16, 3560–3571.

Kitoh, A., Endo, H., Krishna Kumar, K., Cavalcanti, I.F.A., Goswami, P., Zhou, T., 2013. Monsoons in a changing world: a regional perspective in a global context. J. Geophys. Res. 118. http://dx.doi.org/10.1002/jgrd.50258.
Klein Tank, A.M.G., Können, G.P., 2003. Trends in indices of daily temperature and precipitation extremes in Europe, 1946–99. J. Clim. 16, 3665–3680.
Klein Tank, A.M.G., Peterson, T.C., Quadir, D.A., Dorji, S., Zou, X., Tang, H., Santhosh, K., Joshi, U.R., Jaswal, A.K., Kolli, R.K., Sikder, A.B., Deshpande, N.R., Revadekar, J.V., Yeleuova, K., Vandasheva, S., Faleyeva, M., Gomboluudev, P., Budhathoki, K.P., Hussain, A., Afzaal, M., Chandrapala, L., Anvar, H., Amanmurad, D., Asanova, V.S., Jones, P.D., New, M.G., Spektorman, T., 2006. Changes in daily temperature and precipitation extremes in Central and South Asia. J. Geophys. Res. 111, D16105. http://dx.doi.org/10.1029/2005JD006316.
Krishnamurthy, L., Krishnamurthy, V., 2013. Decadal Scale Oscillations and Trend in the Indian Monsoon Rainfall. COLA Technical Report 322. Center for Ocean-Land-Atmosphere Studies, Fairfax, VA.
Krishnan, R., Ramesh, K.V., Samala, B.K., Meyers, G., Slingo, J.M., Fennessy, M.J., 2006. Indian ocean-monsoon coupled interactions and impending monsoon droughts. Geophys. Res. Lett. 33, L08711. http://dx.doi.org/10.1029/2006GL025811.
Krishnan, R., Sabin, T., Ayantika, D., Kitoh, A., Sugi, M., Murakami, H., Turner, A., Slingo, J., Rajendran, K., 2013. Will the south Asian monsoon overturning circulation stabilize any further? Clim. Dyn. 40, 187–211.
Kulkarni, M.A., Singh, A., Mohanty, U.C., 2012. Effect of spatial correlation on regional trends in rain events over India. Theor. Appl. Climatol. 109, 497–505.
Kunkel, K.E., Easterling, D.R., Redmond, K., Hubbard, K., 2003. Temporal variations of extreme precipitation events in the United States: 1895–2000. Geophys. Res. Lett. 30, 1900. http://dx.doi.org/10.1029/2003GL018052.
Lau, W.K.M., Kim, K.-M., 2010. Finger printing the impacts of aerosols on long-term trends of the Indian summer monsoon regional rainfall. Geophys. Res. Lett. 37, L16705. http://dx.doi.org/10.1029/2010GL043255.
Libiseller, C., Grimvall, A., 2002. Performance of partial Mann–Kendall tests for trend detection in the presence of covariates. Environmetrics 13, 71–84.
Moberg, A., Jones, P.D., Lister, D., Walther, A., Brunet, M., Jacobeit, J., Alexander, L.V., Della-Marta, P.M., Luterbacher, J., Yiou, P., Chen, D., Klein Tank, A.M.G., Saladié, O., Sigró, J., Aguilar, E., Alexandersson, H., Almarza, C., Auer, I., Barriendos, M., Begert, M., Bergstrom, H., Öbohm, R., Butler, C.J., Caesar, J., Drebs, A., Founda, D., Gerstengarbe, F.W., Micela, G., Maugeri, M., Österle, H., Pandzic, K., Petrakis, M., Srnec, L., Tolasz, R., Tuomenvirta, H., Werner, P.C., Linderholm, H., Philipp, A., Wanner, H., Xoplaki, E., 2006. Indices for daily temperature and precipitation extremes in Europe analyzed for the period 1901–2000. J. Geophys. Res. 111, D22106. http://dx.doi.org/10.1029/2006JD007103.
Panda, D.K., Kumar, A., 2014. The changing characteristics of monsoon rainfall in India during 1971–2005 and links with large scale circulation. Int. J. Climatol. 34, 3881–3899.
Panda, D.K., Wahr, J., 2016. Spatiotemporal evolution of water storage changes in India from the updated GRACE-derived gravity records. Water Resour. Res. 52, 135–149. http://dx.doi.org/10.1002/2015WR017797.
Panda, D.K., Kumar, A., Singandhupe, R.B., Sahoo, N., 2013. Hydroclimatic changes in a climate-sensitive tropical region. Int. J. Climatol. 33, 1633–1645.
Patra, J.P., Mishra, A., Singh, R., Raghuwanshi, N.S., 2012. Detecting rainfall trends in twentieth century (1871–2006) over Orissa state, India. Clim. Chang. 111 (3), 801–817.
Pingale, S.M., Khare, D., Jat, M.K., Adamowski, J., 2014. Spatial and temporal trends of mean and extreme rainfall and temperature for the 33 urban centers of the arid and semi-arid state of Rajasthan, India. Atmos. Res. 138, 73–90.
Rajeevan, M., Bhate, J., Jaswal, A., 2008. Analysis of variability and trends of extreme rainfall events over India using 104 years of gridded daily rainfall data. Geophys. Res. Lett. 35, L18707. http://dx.doi.org/10.1029/2008GL035143.
Ramesh Kumar, M.R., Krishnan, R., Sankar, S., Unnikrishnan, A.S., Pai, D.S., 2009. Increasing trend of 'Break-Monsoon' conditions over India — role of ocean atmosphere processes in the Indian Ocean. IEEE Geosci. Remote Sens. Lett. 6 (2), 332–336.
Revadekar, J.V., Preethi, B., 2012. Statistical analysis of the relationship between summer monsoon precipitation extremes and food grain yield over India. Int. J. Climatol. 32, 419–429.
Saha, A., Ghosh, S., Sahana, A., Rao, E., 2014. Failure of CMIP5 climate models in simulating post-1950 decreasing trend of Indian monsoon. Geophys. Res. Lett. 41, 7323–7330.
Schmidli, J., Frei, C., 2005. Trends of heavy precipitation and wet and dry spells in Switzerland during the 20th century. Int. J. Climatol. 25, 753–771.
Sen Roy, S., Balling, R.C., 2004. Trends in extreme daily precipitation indices in India. Int. J. Climatol. 24, 457–466.
Singh, V., Goyal, M.K., 2016. Analysis and trends of precipitation lapse rate and extreme indices over North Sikkim eastern Himalayas under CMIP5ESM-2 M RCPs experiments. Atmos. Res. 167, 34–60.
Singh, D., Tsiang, M., Rajaratnam, B., Diffenbaugh, N.S., 2014. Observed changes in extreme wet and dry spells during the south Asian summer monsoon season. Nat. Clim. Chang. 4, 456–461. http://dx.doi.org/10.1038/NCLIMATE2208.
Smith, T.M., Reynolds, R.W., Peterson, T.C., Lawrimore, J., 2008. Improvements to NOAA's historical merged land-ocean surface temperature analysis (1880–2006). J. Clim. 21, 2283–2296.
Sneyers, R., 1999. On the Statistical Analysis of Series of Observations. Technical Note 143, WMO-No 415 Vol. 192.
Stocker, T.F., Qin, D., Plattner, G.-K., Tignor, M., Allen, S.K., Boschung, J., Nauels, A., Xia, Y., Bex, V., Midgley, P.M., 2013. Climate Change 2013: The Physical Science Basis, Intergovernmental Panel on Climate Change. Working Group I Contribution to the IPCC Fifth Assessment Report (AR5). Cambridge Univ. Press, New York.
Subash, N., Singh, S.S., Priya, N., 2011. Variability of rainfall and effective onset and length of the monsoon season over a sub-humid climatic environment. Atmos. Res. 99, 479–487.
Sun, W., Mu, X., Song, X., Wu, D., Cheng, A., Qiu, B., 2016. Changes in extreme temperature and precipitation events in the loess plateau (China) during 1960–2013 under global warming. Atmos. Res. 167, 34–60.
Turner, A.G., Annamalai, H., 2012. Climate change and the south Asian summer monsoon. Nat. Clim. Chang. 2, 587–595.
Villafuerte II, M.Q., Matsumoto, J., Kubota, H., 2015. Changes in extreme rainfall in the Philippines (1911–2010) linked to global mean temperature and ENSO. Int. J. Climatol. 35, 2033–2044. http://dx.doi.org/10.1002/joc.4105.
Vincent, L.A., Zhang, X., Brown, R.D., Feng, Y., Mekis, E., Milewska, E.J., Wan, H., Wang, X.L., 2015. Observed trends in Canada's climate and influence of low-frequency variability modes. J. Clim. 28, 4545–4560.
Vittal, H., Karmakar, S., Ghosh, S., 2013. Diametric changes in trends and patterns of extreme rainfall over India from pre-1950 to post-1950. Geophys. Res. Lett. 40, 3253–3258. http://dx.doi.org/10.1002/grl.50631.
Wang, B., Liu, Y., Kim, H.-J., Webster, P.J., Yim, S.-Y., 2012. Recent change of the global monsoon precipitation (1979–2008). Clim. Dyn. 39, 1123–1135.
Westra, S., Alexander, L.V., Zwiers, F.W., 2013. Global increasing trends in annual maximum daily precipitation. J. Clim. 26, 3904–3918.
Yao, C., Yang, S., Qian, W.H., Lin, Z.M., 2008. Regional summer precipitation events in Asia and their changes in the past decades. J. Geophys. Res. 113, D17107. http://dx.doi.org/10.1029/2007JD009603.
Yue, S., Pilon, P., Phinney, B., Cavadias, G., 2002. The influence of autocorrelation on the ability to detect trend in hydrological series. Hydrol. Process. 16 (9), 1807–1829.
Zhang, L., Zhou, T., 2011. An assessment of monsoon precipitation changes during 1901–2001. Clim. Dyn. 37, 279–296.
Zhang, X., Hervey, K.D., Hogg, W.D., Yuzyk, T.R., 2001. Trends in Canadian stream flow. Water Resour. Res. 37, 987–998.
Zhang, X., Alexander, L., Hegerl, G.C., Jones, P., Klein Tank, A., Peterson, T.C., Trewin, B., Zwiers, F.W., 2011. Indices for monitoring changes in extremes based on daily temperature and precipitation data. WIREs Clim. Change 2, 851–870. http://dx.doi.org/10.1002/wcc.147.
Zhang, X., Wan, H., Zwiers, F.W., Hegerl, G.C., Min, S.K., 2013. Attributing intensification of precipitation extremes to human influence. Geophys. Res. Lett. 40, 5252–5257. http://dx.doi.org/10.1002/grl.51010.
Zhou, T., Yu, R., Li, H., Wang, B., 2008. Ocean forcing to changes in global monsoon precipitation over recent half-century. J. Clim. 21, 3833–3852.
Zolina, O., Simmer, C., Kapala, A., Bachner, S., Gulev, S., Maechel, H., 2008. Seasonally dependent changes of precipitation extremes over Germany since 1950 from a very dense observational network. J. Geophys. Res. 113, D06110. http://dx.doi.org/10.1029/2007JD008393.